A Compact Wideband Circularly Polarized Planar Monopole Antenna with Axial Ratio Bandwidth Entirely Encompassing the Antenna Bandwidth

Falih M. Alnahwi [1], Yasir I. A. Al-Yasir [2,3], Nazar T. Ali [2,4], Ibrahim Gharbia[2], Chan Hwang See [5], and Raed A. Abd-Alhameed [2,6]

[1]Department of Electrical Engineering, College of Engineering, University of Basrah, Basrah, 61001 Iraq
[2]Faculty of Engineering and Informatics, University of Bradford, Bradford BD7 1DP, UK
[3]Skyrora Ltd., Glasgow G68 9LD, UK
[4]Khalifa University, United Arab Emirates
[5]School of Engineering and the Built Environment, Edinburgh Napier University, Edinburgh EH10 5DT, UK
[6]Department of Information and Communication Engineering, Basrah University College of Science and Technology, Basra 61004, Iraq

Corresponding author: r.a.a.abd@bradford.ac.uk

ABSTRACT The antenna presented in this study is a compact wideband monopole with wideband circular polarization that can be used across the whole antenna bandwidth. A rectangular C-shaped patch is partially covered by a ground plane in the proposed planar monopole antenna. Inserting a rectangular stub to the ground plane, etching a slit at the antenna patch, and adding a semicircular stub at the top of the antenna feed line increase the antenna impedance bandwidth (BW) and axial ratio bandwidth (ARBW). An FR4 substrate with overall dimensions of 25 mm×25 mm×1.6 mm is used to create the antenna. The antenna's observed impedance BW is 70% (4.55 GHz in the 4.3-8.85 GHz band), while the measured broadside ARBW is improved to a value of 82.2 percent (5.3 GHz along the range 3.8-9.1 GHz). The impedance BW is perfectly covered by the ARBW; hence the antenna can be considered circularly polarized throughout its operational spectrum. Within the antenna BW, the measured gain is greater than 1.5 dB.

INDEX TERMS Axial Ratio, circular polarization, planar antenna, wideband.

I. INTRODUCTION

The significance of the circular polarization (CP) resides in its noticeable reduction of the multipath interference and its mitigation of the polarization mismatching [1, 2]. Consequently, many planar and non-planar antenna structures have been proposed to exploit these outstanding features of the CP. Recently, CP is utilized for many wireless applications such as WLAN, WiMAX, some satellite applications, and so on. Therefore, antennas with CP are indispensable in such kinds of applications, so it is essential to delve in designing multiband and broadband CP antennas to meet the requirement of each application by using a single antenna.

There are many attempts for designing antennas with CP to concur the aforementioned specifications. Some of the modern trials focus on designing a dual narrow band CP [3] and tri-band CP [4, 5], while the others are oriented toward the design of compact planar antennas with broadband and wideband CP which is the main theme of this work. A broadband CP was generated by incorporation a coplanar feeding with a special wide slot [6], whereas a modified version of the same wide slot antenna was incorporated with a microstrip feeding to generate a broadband CP for C-band applications [7]. A miniaturized CP wide slot antenna with antipodal Y-strip was designed to generate an Axial Ratio Bandwidth (ARBW) equal to 2 GHz [8]. A cross-shaped planar monopole antenna with a ground plane extension was proposed to improve ARBW to 2.6 GHz [9]. The ARBW was further enhanced to 4.2 GHz in [10] by composing an inverted L-shaped tuning stub with a rectangular wide slot whose surface current was

perturbed by some slots and two parallel stubs. Moreover, a three-dimensional printed antenna was designed to realize a tunable wideband CP characteristic with the aid of varactor diodes [11]. A square slot antenna with perturbation element and inverted L-shaped tuning stub was used for ARBW coverage of 2.58-4.74 GHz [12]. A cavity-backed aperture antenna was proposed to improve ARBW and the peak gain over the frequency band from 4.8 to 7.4 GHz [13]. In [14], a new analysis method based on the 3D AR pattern is proposed to generate broadband ARBW. The C-shaped radiator was also utilized to generate 106.3% after adding two inclinations in the ground plane [15]. More recently, a loaded strip was attached to a square slot to broaden ARBW to 75.1% and covered the entire antenna -10dB bandwidth [16].

All the above mentioned broadband antennas (except [16]) have -10dB impedance bandwidth (BW) that exceeds the ARBW. In other words, the CP does not cover the entire bandwidth of the antenna in the mentioned papers. In addition, the antenna size in [16] is relatively large with respect to the covered frequency range. Therefore, a miniaturized planar antenna with wideband CP that entirely covers the -10dB bandwidth is intended to be designed in this work to fill in this knowledge gap

In this paper, a compact wideband circularly polarized planar antenna with C-shaped patch that is partially covered by the ground plane is presented. A noticeable improvement in the impedance BW and the broadside ARBW is achieved by etching a slit on the antenna patch, attaching a rectangular stub to ground plane, and attaching a semicircular stub at the upper terminal of the feed line. 100% of the antenna BW can be utilized for CP applications because the ARBW fully covers the antenna impedance BW in spite of the antenna compact size. The measured results are well agreed with the simulated results, and both show wide impedance BW and ARBW with very acceptable gain value and comparable size.

II. ANTENNA STRUCTURE

Fig. 1 illustrates the geometry of the proposed wideband antenna with the optimized values of each parameter. The antenna is engraved on an FR4 dielectric substrate with dielectric constant of $\varepsilon_r = 4.3$, loss tangent of 0.025, and height of $h = 1.6$ mm. The overall dimensions of the antenna is equal to 25 mm × 25 mm × 1.6 mm. This is equivalent to $0.37\,\lambda \times 0.37\,\lambda \times 0.024\,\lambda$ at its lower operating frequency band. To form a wideband planar monopole antenna, the general antenna structure is made of a 50Ω microstrip feed line connected to a C-shaped patch which represents a very perfect CP structure to be started with [17, 18]. A stub with length equal to L_{st} has been attached to the ground plane to improve the ARBW of the proposed antenna. Further enhancement in the ARBW has been acquired after engraving a slit with length equal to L_s on the patch of the proposed antenna in addition to attaching a semicircular stub with radius r at the top of the feed line.
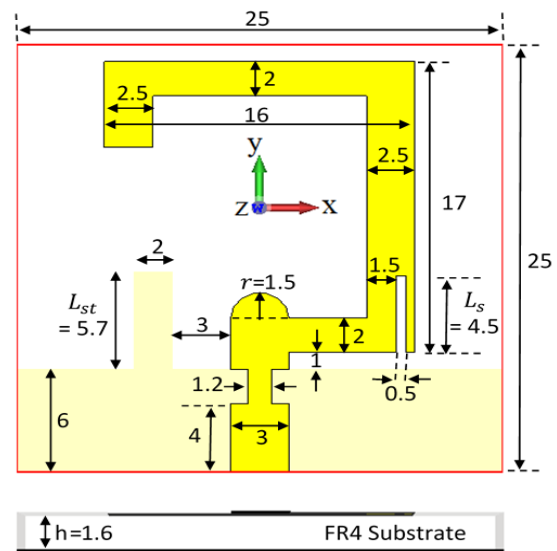

FIGURE 1. The geometry of the proposed antenna (all dimensions are in mm)

III. DESIGN PROCEDURE

The procedure that has been followed until obtaining the final structure (Ant.1-4) is demonstrated in Fig. 2, while the resulted reflection coefficient (S_{11}) and the AR corresponding to each structure is exhibited in Fig. 3 with the aid of CST Microwave Studio simulation suite. Ant.1 represents a conventional C-shaped monopole antenna, which has two orthogonal paths with slightly different lengths to form two slightly separated resonant frequencies.
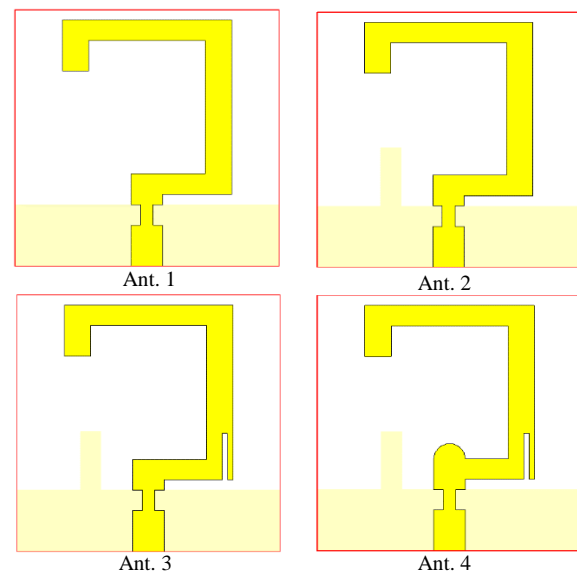

FIGURE 2. The design procedure of the proposed antenna.

IEEE *Access*

As claimed in [1], these two slightly separated orthogonal resonations results in a radiation with CP. The resulted antenna -10dB bandwidth is equal to 2.6 GHz, and the 3dB ARBW is equal to 1.3 GHz as shown in Fig. 3. Ant.2 includes the presence of a rectangular stub in the ground plane. The contribution of this structure is enormous in the improvement of the -10dB bandwidth (which is reached to value equal to 5.6 GHz) because the stub adds an additional resonant frequency at 9.3 GHz. The position of the second resonant frequency is modified, and it results in 3dB ARBW equal to 2.5 GHz as depicted in Fig. 3. However, the 3dB ARBW has witnessed a subtle improvement because the additional frequency does not contribute with the other resonant frequencies to form a CP. In Ant.3, the presence of the slit modifies the separation between the first and second resonant frequencies because it elongates the horizontal electrical length of the antenna current path. Therefore, it results in an improvement in the 3dB ARBW up to 2.8 GHz, but the slit reduces the antenna -10dB impedance BW to 4.2 GHz because the slit causes a mismatching in the third resonant frequency.
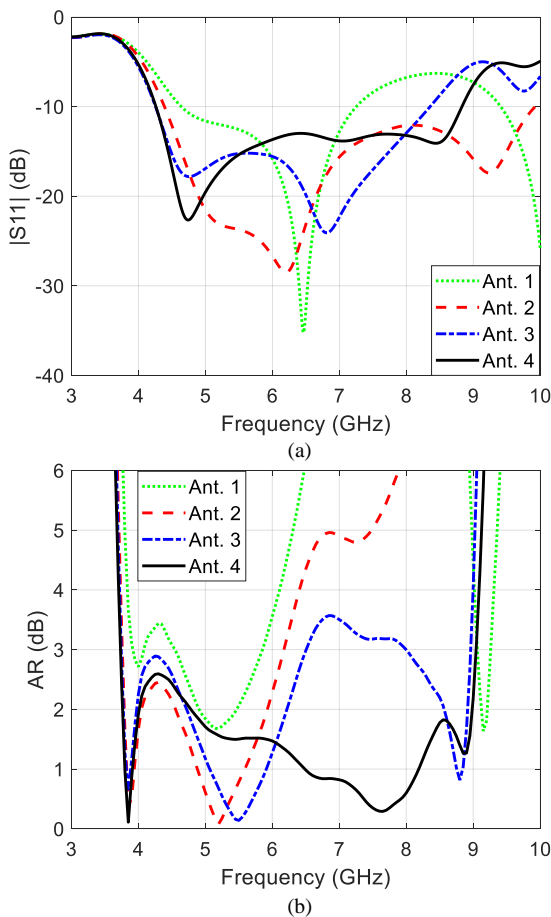
Ant. 4 exploits the mismatched resonant frequency to form a CP whose ARBW surpasses the -10dB impedance BW of the antenna. This has been achieved by engraving the semicircular stub which modifies the horizontal current path of the antenna in such a way that provides an additional resonant frequency at 8.5 GHz. This resonant frequency plays a vital role with the mismatched frequency centered at 9.6 GHz in generating two orthogonal resonances with slight separation. Therefore, the 3dB ARBW is improved at the upper-frequency coverage of the antenna to form an overall frequency coverage equal to 5.3 GHz (3.7-9 GHz). The overall -10dB impedance BW is 4.6 GHz (4.2-8.8 GHz). It can clearly be seen that the ARBW perfectly covers the entire -10dB antenna bandwidth, so it can be said that the antenna has a perfect coverage of CP because the entire bandwidth operates under the CP condition.

To verify the CP behavior of the antenna as in [18, 19], the current distribution of the proposed antenna at 4.7 GHz is illustrated in Fig. 4. This figure shows the antenna surface current at different time instants. The rotation of the current can clearly be seen, and it shows a Right Hand Circular Polarization (RHCP) with respect to the positive z-axis. It is worth mentioning that the LHCP can be obtained by mirroring the antenna structure with respect to the y-axis.
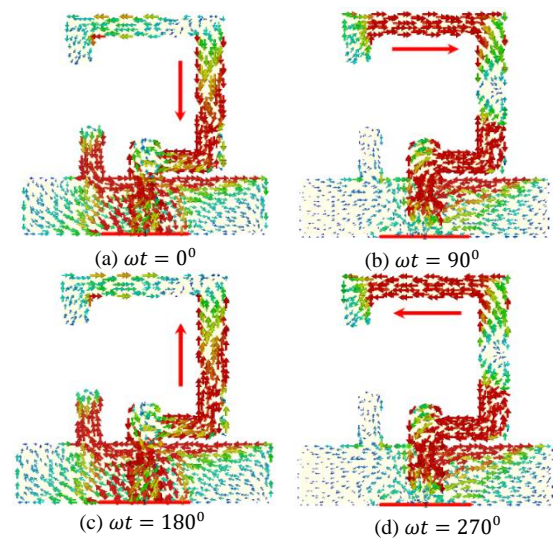

(a) $\omega t = 0^0$ (b) $\omega t = 90^0$

(c) $\omega t = 180^0$ (d) $\omega t = 270^0$

FIGURE 4. Current distribution of the proposed antenna with RHCP at 4.7GHz and different time instants.

IV. PARAMETRIC STUDY

This section studies the effect of sensitive parameters, i.e. stub length (L_{st}), slit length (L_s) and radius of semicircular stub (r), that contribute to the generation of the CP behavior. As mentioned in the previous section, the rectangular stub improves the -10dB BW to a value equal to 5.6 GHz because the stub adds an additional resonant frequency at 9.3 GHz. The position of the second resonant frequency is modified, and it results in 3dB ARBW equal to 2.5 GHz. However, its effect on the 3dB ARBW is subtle because the additional frequency does not contribute to the other resonant frequencies to form a

FIGURE 3. Simulation results of Ant. 1-4: (a) reflection coefficient and (b) Axial Ratio.

CP. On the other hand, the presence of the slit modifies the separation between the first and second resonant frequencies because it elongates the horizontal electrical length of the antenna current path. Therefore, it results in an improvement in the 3dB ARBW up to 2.8 GHz, but the slit reduces the antenna -10dB impedance BW to 4.2 GHz because the slit causes a mismatching in the third resonant frequency. Finally, the semicircular stub exploits a mismatched resonant frequency at 9.6 GHz to form a CP whose ARBW surpasses the -10dB impedance BW of the antenna because it modifies the horizontal current path of the antenna in such a way that provides an additional resonant frequency at 8.5 GHz. Therefore, the 3dB ARBW is improved at the upper-frequency coverage of the antenna to form an overall frequency coverage equal to 5.3 GHz (3.7-9 GHz).

Fig. 5 illustrates the effect of the stub length (L_{st}) that is attached to the ground plane on the antenna reflection coefficient and the AR. This parameter affects the location of the second resonant which directly affects the CP at the lower frequency range of the antenna. It is found that $L_{st} = 5.7mm$ provides the widest -10dB BW and 3dB ARBW.
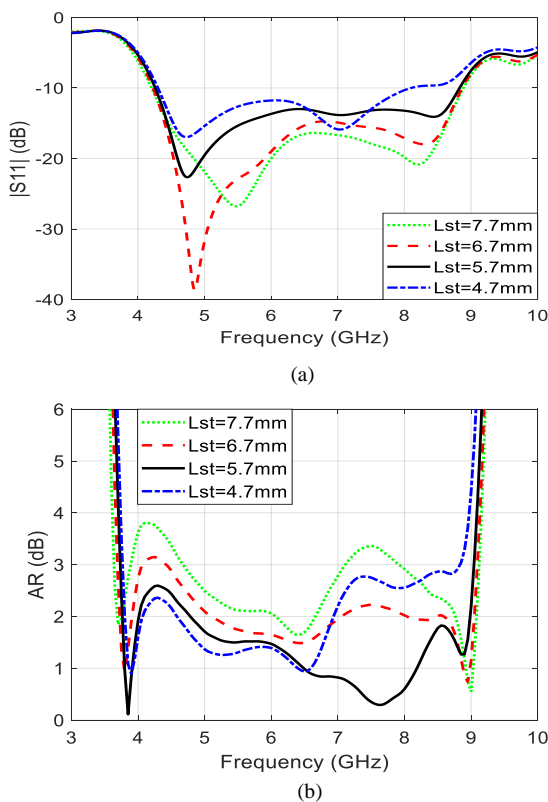
separation between the third and fourth resonant frequency that leads to the widest -10dB bandwidth and 3dB ARBW. The effect of the semicircular stub whose radius is equal to (r) is illustrated in Fig. 7. This parameter is responsible for the showing up of the third resonant frequency, so it significantly affects the CP behavior of the upper side band of the proposed antenna. $r = 1.5mm$ results in a perfect separation between the third resonant frequency and the mismatched fourth resonant frequency which results in the widest -10dB impedance BW and the 3dB ARBW.
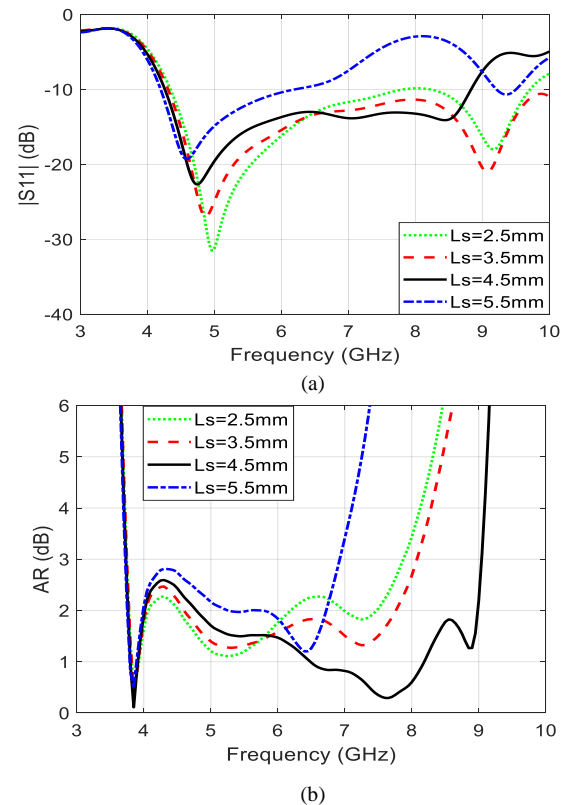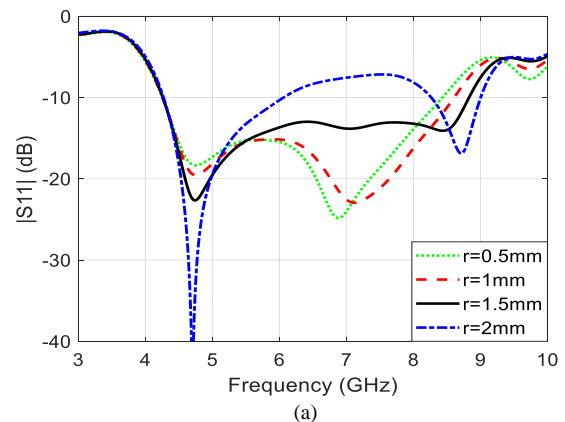

(a)

(b)

FIGURE 6. Simulation results of the proposed antenna at $L_{st} = 5.7mm$, $r = 1.5mm$, and different values of L_s: (a) reflection coefficient and (b) Axial Ratio.

(a)

(b)

FIGURE 5. Simulation results of the proposed antenna at $L_s = 4.5mm$, $r = 1.5mm$, and different values of L_{st}: (a) reflection coefficient and (b) Axial Ratio.

Fig. 6 reveals the effect of changing the slit length (L_s) on the antenna reflection coefficient and the AR as a function of frequency. This parameter modifies the location of the third resonant frequency. $L_s = 4.5\ mm$ gives the optimum

(a)

(b)

FIGURE 7. Simulation results of the proposed antenna at $L_{st} = 5.7mm$, $L_s = 4.5mm$, and different values of r: (a) reflection coefficient and (b) Axial Ratio.
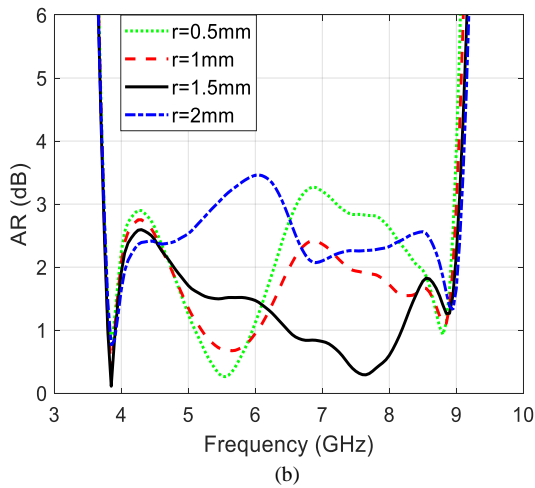
V. MEASURED RESULTS

Fig. 8 exhibits the front and the back view of the prototype of the proposed CP antenna. The measurements were acquired with the aid of Agilent N5242A vector network analyzer and a 100 cubic meter anechoic chamber, at the University of Bradford/Faculty of Engineering and Informatics. The simulated and measured reflection coefficients and ARs as a function of frequency are shown in Fig. 9. This figure shows a simulated -10dB impedance BW equal to 4.6 GHz (70.8%) along the range (4.2-8.8 GHz) and simulated 3dB ARBW equal to 5.3 GHz (83.5%) along the range (3.7-9 GHz). On the other hand, the measured reflection coefficient and AR show -10dB impedance BW equal to 4.55 GHz (70%) along the range (4.3-8.85 GHz) and 3dB ARBW equal to 5.3 GHz (82.2%) along the range (3.8-9.1 GHz). It is clear from this figure that the -10dB impedance BW is perfectly covered by the 3dB ARBW. Therefore, it can be said that the antenna is a CP antenna over the entire operating bandwidth. Consequently, we propose a new coefficient named (The Effective CP Percentage with Respect to the Antenna Bandwidth), and it can be denoted by ($ECP\%$) as in [16]. This coefficient measures the amount of the antenna bandwidth that can be utilized for CP applications, and it can be given by (1):

$$ECP\% = (((-10dB\ BW) \cap (3dB\ ARBW))/(-10dB\ BW)) \times 100\% \quad (1)$$

where $-10dB\ BW$ and $3dB\ ARBW$ represent the -10dB impedance BW and the 3dB axial ratio bandwidth, respectively. The symbol ($\cap$) denotes the intersection between the two bandwidths. In the proposed design, the value of the $ECR\%$ is equal to 100% since the intersection between the two bandwidths is equal to the value of the -10dB bandwidth.
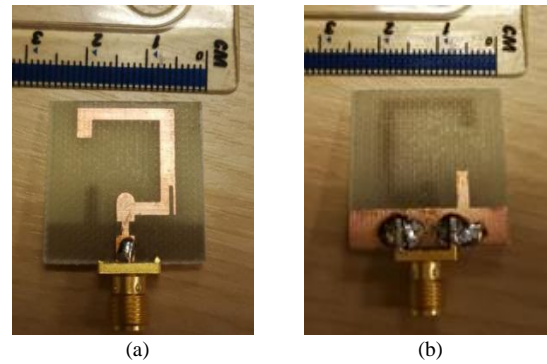

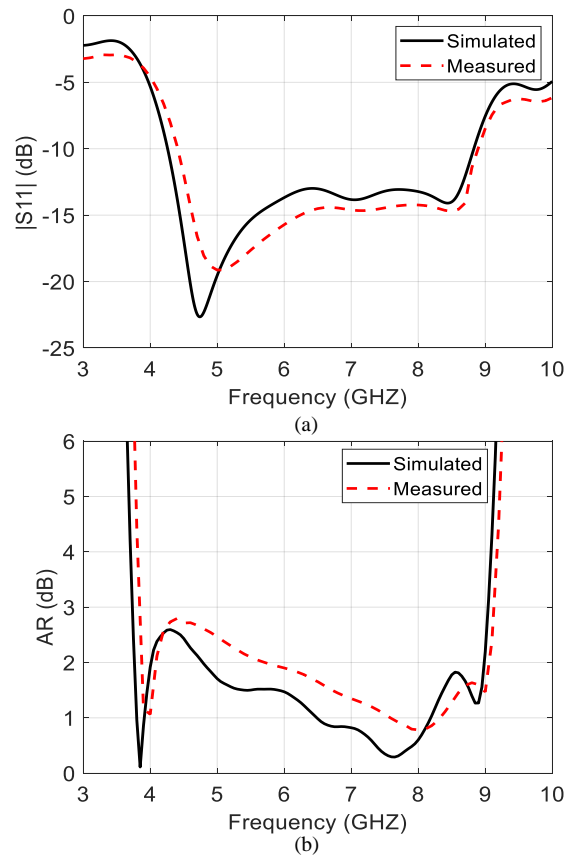**FIGURE 8.** The prototype of the proposed antenna (a) front view and (b) back view.

FIGURE 9. The antenna results as a function of frequency (a) reflection coefficient and (b) axial ratio.

In order to demonstrate the radiation characteristics of the proposed antenna, the antenna gain and the normalized power patterns at the antenna resonant frequencies are illustrated in Fig. 10 and 11, respectively. The antenna has very satisfactory gain values over the entire operating band. Fig. 11 illustrates the co-polarized and cross-polarized radiation patterns of the antenna in the XZ- and YZ- planes at the resonant frequencies

of the antenna. It is clear that the values of the co- and cross-polarized patterns are close to each other (with a difference of less than 3dB) in the broadside direction of the antenna at the three resonant frequencies, and this verifies the presence of the CP in the broadside direction. As future work, the antenna will be attached by a suitable reflector positioned at its back side to get rid of the undesired back radiation. The deviation between the measured and simulated results may be attributed to the fabrication imperfection, imperfect soldering of the SMA connector, and the reflections caused by the surrounding objects inside the anechoic chamber.
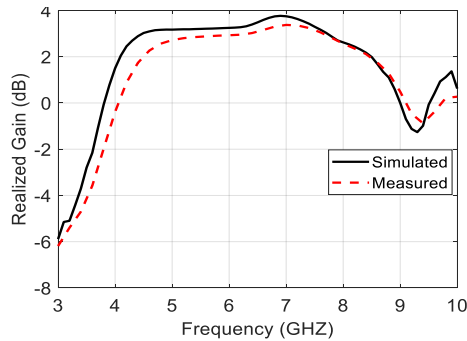

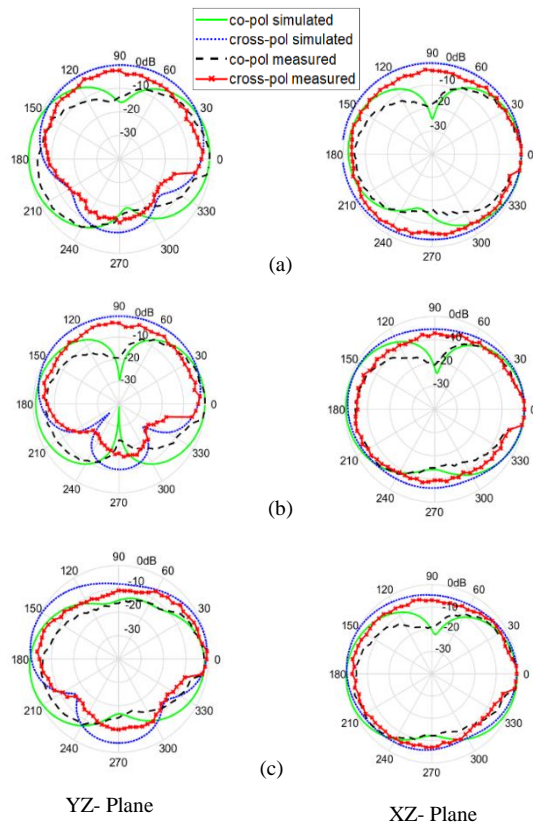**FIGURE 10. Simulated realized gain of the proposed antenna as a function of frequency.**

FIGURE 11. The co-polarized and cross-polarized radiation patterns of the proposed antenna at (a) f=4.7 GHz, (b) f=7 GHz, and (c) f=8.5 GHz.

Table I demonstrates a comparison between the proposed antenna with other published designs in term of antenna size, fractional -10dB impedance BW, fractional 3dB ARBW, and ECP%. It is worth to mention that the antenna dimensions are calculated with respect to the wavelength (λ) corresponding to the lower operating frequency. It is clear from this table that the previous works has a value of ECP% less than 100% except reference [16]. However, the proposed design surpasses that of [16] by its small dimensions and wide -10dB BW and 3dB ARBW.

TABLE I

A COMPARISON BETWEEN THE PROPOSED ANTENNA AND OTHER DESIGNS, WHERE λ DENOTES THE WAVELENGTH CORRESPONDING TO THE LOWER OPERATING FREQUENCY

Ref.	Ant. Dimensions	-10 dB BW %	3 dB ARBW %	ECP %
[6]	$0.4 \lambda \times 0.4 \lambda \times 0.01 \lambda$	101	52	51.5
[7]	$0.3 \lambda \times 0.3 \lambda \times 0.019 \lambda$	90.2	40	43.4
[8]	$0.4 \lambda \times 0.4 \lambda \times 0.024 \lambda$	84	41.3	49.2
[9]	$0.6 \lambda \times 0.6 \lambda \times 0.013 \lambda$	92.7	54.2	58.5
[10]	$0.3 \lambda \times 0.24 \lambda \times 0.015 \lambda$	55.5	42.6	76.8
[12]	$0.7 \lambda \times 0.7 \lambda \times 0.016 \lambda$	69.2	59	85.3
[13]	$0.8 \lambda \times 0.8 \lambda \times 0.3 \lambda$	70	43.3	61.9
[15]	$0.33 \lambda \times 0.37 \lambda \times 0.012 \lambda$	106.3	104.7	92
[16]	$0.8 \lambda \times 0.8 \lambda \times 0.016 \lambda$	65.8	75.1	100
This Work	$0.37\lambda \times 0.37\lambda \times 0.024\lambda$	70	82.2	100

VI. CONCLUSION

This work successfully designs a compact C-shaped wideband planar monopole antenna with wideband CP. An FR4 substrate with a dielectric constant of 4.3, a loss tangent of 0.025, and dimensions of 0.37 λ×0.37 λ×0.024 λ is used to create the antenna. The antenna's measured impedance BW is 4.55 GHz over a frequency range of 4.3-8.85 GHz (70%), whereas the measured broadside ARBW is 5.3 GHz over a frequency range of 3.8-9.1 GHz (82.2%). Along its impedance BW, the proposed antenna can be utilized for CP applications because the ARBW perfectly encompasses the entire antenna bandwidth. The measurements also show gain values larger than 1.5 dB within the antenna BW. As a future work, the antenna will be attached by a suitable reflector positioned at its back side to get rid of the undesired back radiation and enhance the peak gain of the antenna.

ACKNOWLEDGMENT

REFERENCES

[1] K.-L. Wong, *Compact and Broadband Microstrip Antennas* (Wiley Series in Microwave and Optical Engineering). New York, NY, USA: Wiley, 2002.

[2] C. A. Balanis, *Antenna theory : analysis and design*. New Jersey, NJ, USA: John Wiley and Sons, 2016.

[3] N. Evans, Y. X. Liu, L. Shafai, and D. Isleifson, "Capacitively Coupled Single-Layer Dual-Band Circularly Polarized GPS Ring Antennas," (in English), *2021 Ieee 19th International Symposium on Antenna Technology and Applied Electromagnetics (Antem),* 2021.

[4] E. Z. Zhang, A. Michel, P. Nepa, and J. H. Qiu, "Multifeed tri-band circularly polarized antenna for UHF/MW-RFID application," (in English), *International Journal of Rf and Microwave Computer-Aided Engineering,* vol. 32, no. 1, Jan 2022.

[5] I. Fatima, A. Ahmad, S. Ali, M. Ali, and M. Iram Baig, "Triple-Band Circular Polarized Antenna for Wlan/Wi-Fi/Bluetooth/Wimax Applications," *Progress In Electromagnetics Research C,* vol. 109, pp. 65-75, 2021.

[6] Z. F. Chen, B. Xu, J. Hu, and S. L. He, "A CPW-fed broadband circularly polarized wide slot antenna with modified shape of slot and modified feeding structure," (in English), *Microwave and Optical Technology Letters,* vol. 58, no. 6, pp. 1453-1457, Jun 2016.

[7] M. S. Ellis, Z. Q. Zhao, J. N. Wu, X. X. Ding, Z. P. Nie, and Q. H. Liu, "A Novel Simple and Compact Microstrip-Fed Circularly Polarized Wide Slot Antenna With Wide Axial Ratio Bandwidth for C-Band Applications," (in English), *Ieee Transactions on Antennas and Propagation,* vol. 64, no. 4, pp. 1552-1555, Apr 2016.

[8] M. Nosrati and N. Tavassolian, "Miniaturized Circularly Polarized Square Slot Antenna With Enhanced Axial-Ratio Bandwidth Using an Antipodal Y-strip," (in English), *Ieee Antennas and Wireless Propagation Letters,* vol. 16, pp. 817-820, 2017.

[9] K. O. Gyasi *et al.*, "A Compact Broadband Cross-Shaped Circularly Polarized Planar Monopole Antenna With a Ground Plane Extension," (in English), *Ieee Antennas and Wireless Propagation Letters,* vol. 17, no. 2, pp. 335-338, Feb 2018.

[10] L. Wang, W. X. Fang, Y. F. En, Y. Huang, W. H. Shao, and B. Yao, "A new broadband circularly polarized square-slot antenna with low axial ratios," (in English), *International Journal of Rf and Microwave Computer-Aided Engineering,* vol. 29, no. 1, Jan 2019.

[11] M. F. Farooaui and A. Kishk, "3-D-Printed Tunable Circularly Polarized Microstrip Patch Antenna," (in English), *Ieee Antennas and Wireless Propagation Letters,* vol. 18, no. 7, pp. 1429-1432, Jul 2019.

[12] L. C. Hao, C. Q. Fan, H. Wang, B. Li, and W. T. Yin, "Novel square slot circularly polarized antenna with broadband characteristics," (in English), *International Journal of Rf and Microwave Computer-Aided Engineering,* vol. 32, no. 1, Jan 2022.

[13] W. W. Yang and J. Y. Zhou, "Wideband Circularly Polarized Cavity-Backed Aperture Antenna With a Parasitic Square Patch," (in English), *Ieee Antennas and Wireless Propagation Letters,* vol. 13, pp. 197-200, 2014.

[14] F. M. Alnahwi, Y. I. A. Al-Yasir, C. H. See, and R. A. Abd-Alhameed, "Single-Element and MIMO Circularly Polarized Microstrip Antennas with Negligible Back Radiation for 5G Mid-Band Handsets," (in English), *Sensors,* vol. 22, no. 8, Apr 2022.

[15] H. Y. Tang, K. Wang, R. M. Wu, C. Yu, J. Zhang, and X. T. Wang, "A Novel Broadband Circularly Polarized Monopole Antenna Based on C-Shaped Radiator," (in English), *Ieee Antennas and Wireless Propagation Letters,* vol. 16, pp. 964-967, 2017.

[16] Y. Liu, S. T. Cai, X. M. Xiong, W. J. Li, and J. Yang, "A novel wideband circularly polarized modified square-slot antenna with loaded strips," (in English), *International Journal of Rf and Microwave Computer-Aided Engineering,* vol. 29, no. 10, Oct 2019.

[17] M. Midya, S. Bhattacharjee, and M. Mitra, "Circularly polarized planar monopole antenna for ultrawideband applications," (in English), *International Journal of Rf and Microwave Computer-Aided Engineering,* vol. 29, no. 11, Nov 2019.

[18] K. Ding, C. Gao, T. Yu, and D. Qu, "Broadband C-Shaped Circularly Polarized Monopole Antenna," *IEEE Transactions on Antennas and Propagation,* vol. 63, no. 2, pp. 785-790, 2015.

[19] M. Midya, S. Bhattacharjee, and M. Mitra, "Broadband Circularly Polarized Planar Monopole Antenna With G-Shaped Parasitic Strip," *IEEE Antennas and Wireless Propagation Letters,* vol. 18, no. 4, pp. 581-585, 2019.

Falih M. Alnahwi received a Ph.D. in Electrical and Computer Engineering from the University of Missouri-Columbia in the United States in 2015, while his B.Sc. and M.Sc. were granted by the University of Basrah in Iraq in 2004 and 2007, respectively. Since he completed his Ph.D, he has joined the faculty members of the Department of Electrical Engineering at the University of Basrah as a Lecturer, and now he is still working there as an Associate Professor and director of graduate students. His field of interest is antennas and wireless propagation especially the multiband, broadband, ultra-wide band antennas, Electromagnetic Fields, MIMO Systems, Metamaterial, Mutual Coupling Reduction Techniques, Reconfigurable Antennas as well as Microwave Filters Design. He also interests the research in Digital Communications, Optimization, and Electromagnetic Compatibility.

Yasir Al-Yasir (Member, IEEE) received the B.Sc. and M.Sc. degrees from the University of Basrah, Iraq, in 2012 and 2015, respectively, and the Ph.D. degree from the University of Bradford, U.K., in 2021. In 2014, he joined the Antennas and RF Engineering research group as a research visitor at the University of Bradford. From 2018 to 2021, he was appointed at the University of Bradford as a Marie Curie Research Fellow in the H2020-ITN-SECRET project funded by EU Commission, targeting 5G mobile small cells. He was working as a Research Fellow in the SATNEX-V project, funded by the European Space Agency. He is also a Reviewer for various high-ranking journals and publishers such as IEEE, IET, Wiley, Springer, Elsevier, and MDPI. Dr Al-Yasir is the recipient and a co-recipient of various awards and prizes such as the Best Paper Award at the IEEE 2nd 5G World Forum and IEEE 4th 5G Summit Dresden, Germany. He has authored 2 books and 10 book chapters and published more than 130 journal and conference papers on aspects of RF and Microwave Engineering. His articles have more than 2100 citations with 25 h-index, reported by the Google Scholar.

Nazar T Ali (M'01SM'03) received a Ph.D. degree in electrical and electronic engineering from the University of Bradford, UK, in 1990. From 1990 to 2000, he held various posts at the University of Bradford as a researcher and lecturer. He worked in many collaborative research projects in the UK under the umbrella of the centre of research excellence, Department of Trade and Industry (DTI) and EPSRC. This involved a consortium of a number of universities and industrial companies. He is currently an associate professor at Khalifa University in the United Arab Emirates. His current research interests include antennas and RF circuits and systems, indoor and outdoor localization techniques, and RF measurements. He has over 100 articles published in peer-reviewed high-quality journals and conferences.

Ibrahim Gharbia earned a Bachelor of Science degree in Electrical and Electronic Engineering from the Department of Electrical and Electronic Engineering at the Subrata Engineering Faculty in Libya in 1997. In the years following his graduation, he held positions as a lecturer in the fields of Computing, Science, and Mathematics. Later, he worked as a research assistant at the Libyan forensic lab, where he was recognised as the best employee in his department. As a result, he was awarded a scholarship to pursue his Master of Science degree at the University of Huddersfield in the United Kingdom, and he was granted this degree in 2012. Training Courses supporting the Digital Evidence Forensic Science were actively pursued at Huddersfield University by the student from 2012 until 2015. 2006 until May of 2012, followed by time spent working for the Catholic Housing Aid Society, as an Interpreter at Bradford from 2015 until 2018, and finally as the Chairperson for the New Libya Society. Following that, he enrolled at Bradford University in order to pursue a doctoral degree in the Radio Frequency Research group there. His areas of expertise include RFID Reader and Tag designs, programming, sensor design, and antenna design. he is also interested in electromagnetic fields and MIMO.
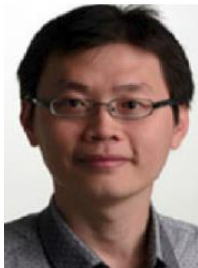
Chan Hwang See (Senior Member, IEEE) received the B.Eng. degree (Hons.) in electronic, telecommunication, and computer engineering and the Ph.D. degree from the University of Bradford, U.K., in 2002 and 2007, respectively. He was a Senior Lecturer (Programme Leader) in electrical and electronic engineering with the School of Engineering, University of Bolton, U.K. He is currently an Associate Professor and the Head of electrical engineering and mathematics with the School of Engineering and the Built Environment, Edinburgh Napier University, U.K. He is also a Visiting Research Fellow with the School of Engineering and Informatics, University of Bradford. Prior to this, he was a Senior Research Fellow with the Antennas and Applied Electromagnetics Research Group, University of Bradford. His research interests include wireless sensor network system design, computational electromagnetism, antennas, and acoustic sensor design. He has published over 200 peer-reviewed journal articles and conference papers in the areas of antennas, computational electromagnetics, microwave circuits, acoustic sensors, and wireless sensor system designs. He is a coauthor for one book and three book chapters. He is a Fellow of the Institution of Engineering and Technology and the Higher Education Academy. He was a recipient of two Young Scientist Awards from the International Union of Radio Science (URSI) and Asia-Pacific Radio Science Conference (AP-RASC) in 2008 and 2010, respectively. He was awarded the Certificate of Excellence for his successful Knowledge Transfer Partnership (KTP) with Yorkshire Water on the design and implementation of a wireless sensor system for sewerage infrastructure monitoring in 2009. He is a Chartered Engineer. He is also an Associate Editor of IEEE ACCESS.

Raed Abd-Alhameed (M'02, SM'13) is currently a Professor of electromagnetic and radiofrequency engineering with the University of Bradford, U.K. He is also the Leader of radiofrequency, propagation, sensor design, and signal processing; in addition to leading the Communications Research Group for years within the School of Engineering and Informatics, University of Bradford. He has long years' research experience in the areas of radio frequency, signal processing, propagations, antennas, and electromagnetic computational techniques. He has published over 800 academic journals and conference papers; in addition, he has co-authored seven books and several book chapters including seven patents. He is a principal investigator for several funded applications to EPSRCs, Innovate UK and the leader of several successful knowledge Transfer Programmes, such as with Arris (previously known as Pace plc), Yorkshire Water plc, Harvard Engineering plc, IETG Ltd., Seven Technologies Group, Emkay Ltd., and Two World Ltd. He has also been a co-investigator in several funded research projects including 1) Horizon 2020 Research and Innovation programme under grant agreement H2020-MSCA-RISE-2019-eBORDER-872878; 2) H2020 MARIE Skªodowska-CURIE ACTIONS: Innovative Training Networks Secure Network Coding for Next Generation Mobile Small Cells 5G-US; 3) European Space Agency: Satellite Network of Experts V, Work Item 2.6: Frequency selectivity in phase-only beamformed user terminal direct radiating arrays; 4) Nonlinear and demodulation mechanisms in biological tissue (Dept. of Health, Mobile Telecommunications & Health Research Programme; and 5) Assessment of the Potential Direct Effects of Cellular Phones on the Nervous System (EU: collaboration with six other major research organizations across Europe). He was a recipient of the Business Innovation Award for his successful KTP with Pace and Datong companies on the design and implementation of MIMO sensor systems and antenna array design for service localizations. He is the chair of several successful workshops on energy-efficient and reconfigurable transceivers: Approach toward Energy Conservation and CO_2 Reduction that addresses the biggest challenges for the future wireless systems. He is also the general chair of the IMDC-IST International Conference since 2020. He is a co-editor for Electronics MDPI Journal since June 2019; in addition, he was a Guest Editor of IET Science, Measurements and Technology Journal since 2009. He has been a Research Visitor of Wrexham University, Wales, since 2009, covering the wireless and communications research areas. His interest in computational methods and optimizations, wireless and mobile communications, sensor design, EMC, beam steering antennas, energy-efficient PAs, and RF predistorter design applications. He is a fellow of the Institution of Engineering and Technology and a fellow of the Higher Education Academy and a Chartered Engineer.